Optical density effects in photon echo experiments

R. W. Olson, H. W. H. Lee, F. G. Patterson, and M. D. Fayer

Department of Chemistry, Stanford University, Stanford, California 94305
(Received 26 June 1981; accepted 14 September 1981)

The effects of optical density (OD) on photon echo experiments is examined both theoretically and experimentally. The theoretical treatment involves coupled Maxwell-Optical Bloch equations, and the experiments are picosecond photon echo studies of the mixed molecular crystal, pentacene in naphthalene. Under high power excitation ($\pi/2, \pi$) in high OD samples, the echo decays are predicted and observed to be faster than decays arising solely from the intrinsic molecular T_2. The increase in the echo decay rate vanishes in the limit of low power or low OD, permitting the intrinsic molecular T_2 to be measured. Previously reported concentration effects are shown to actually be optical density effects. The experimentally determined intrinsic molecular T_2 of pentacene in naphthalene is shown to be independent of concentration and temperature (below ~ 2 K) and $T_2 \neq 2T_1$. It is suggested that the difference between T_2 and $2T_1$ is due to the static multiplet level structure arising from the electronic state-phonon coupling.

I. INTRODUCTION

Optical coherence experiments, such as the photon echo[1] and stimulated photon echo,[2] are often described as direct optical analogs of pulsed magnetic resonance experiments.[3] This depiction is clearly enhanced by the well-known article by Feynmann, Vernon, and Hellwarth.[4] However, in practical application many differences arise between them. For example, in the magnetic resonance case, the sample is small relative to the wavelength of the radiation field, while in the optical case, the sample is large compared to the exciting wavelength. This results in a wave vector matching condition, not found in magnetic resonance, permitting photon echo emission only in a unidirectional coherent pulse.

Additionally, it is possible for the optical sample to absorb a non-negligible fraction of the incident excitation energy, i.e., the sample is optically dense. In such instances, not only is the sample coherently excited by the radiation field, but the induced sample polarization reacts upon the field to a significant extent, altering the total energy and the shape of the excitation pulse (hence the pulse area) as it propagates through the sample. Molecules at different depths in the sample experience different excitation pulse amplitudes and shapes. That this can profoundly affect the results of pulsed optical coherence experiments is a principal theme of this paper. While much work has been done on the effect of the sample upon pulse shapes and pulse evolution,[5] attention has not been directed toward the effects of these same interactions upon the sample and their implications for the use of pulsed optical coherence experiments to extract information about dynamical processes in high optical density samples. These considerations are particularly important in performing photon echoes in high concentration samples, e.g., in looking for the onset of an Anderson transition[6] or in the study of pure crystal exciton states.

The photon echo experiment is a two-excitation-pulse optical coherence experiment. The effect that optical density [$\mathrm{OD} \equiv \log(I_0/I)$] has on the photon echo experiment arises from the fact that pulse areas (whether excitation or echo pulses) change as a function of the distance the pulse has traveled through the sample. This can be related to the loss of energy from a pulse as it leaves excited molecules in its wake and to the reshaping of the pulse as the sample polarization acts back upon the radiation field.

To illustrate these effects, consider the photon echo sequence in an optically dense sample. As the first excitation pulse propagates through the sample, its area decreases so that molecules at different distances into the sample experience different pulse areas, hence undergo different amounts of excitation. The second excitation pulse also undergoes evolution, and again, each point in the sample will experience a different pulse area. In the time interval τ between the excitation pulses, the sample partially relaxes to the ground state. Although the first pulse always encounters a sample with all molecules in the ground state, the second encounters a sample with a different degree of excitation for each value of τ. Since the pulse shaping effects depend on the degree of sample excitation, the evolution of the area of the second excitation pulse is τ dependent. Finally, the echo pulse is generated by polarizations associated with the in-plane components of excitations in different parts of the sample and is attenuated or amplified by a gain factor related to the degree of excitation of the molecules in the path of the echo pulse. Like the second excitation pulse, the echo experiences a τ-dependent interaction as it propagates through the sample. These considerations, when investigated theoretically and experimentally, demonstrate the profound effects an optically dense sample can have on an echo decay. It is important to understand OD effects so that physically meaningful information about the molecular system can be extracted from high OD samples.

In this paper, we will first discuss the coupled Maxwell-Optical Bloch equations used to theoretically examine the role of OD effects in photon echo experiments. We will then present an experimental examination of OD effects on photon echoes in the mixed molecular crystal pentacene in naphthalene. It will be shown that the previously reported dependence of photon echo decay rate on concentration for pentacene in naphthalene[7] (and presumably also for naphthalene in durene[8]) is, in fact,

 0021-9606/82/010031-09$02.10

due to OD effects. We will then demonstrate that OD effects may be overcome by performing photon echoes at very low excitation intensities and that pentacene in naphthalene crystals, regardless of concentration or OD, all exhibit the same low power echo decay time $T_2 \approx 32$ ns. This T_2 is still significantly faster than $2T_1 = 38.4$ ns, where T_1 is the fluorescence lifetime. The experimental results are temperature independent at very low temperatures, implying that $T_2 \neq 2T_1$ at 0 K. Finally, we will discuss recent theoretical work[9] which suggests that $T_2 \neq 2T_1$ can be the general result of photon echo experiments performed on complex systems, i.e., even at 0 K, the echo decay rate is not solely determined by the fluorescence lifetime.

To avoid confusion we will denote the decay time of the photon echo experiment (apparent T_2) with the symbol $T_2^\dagger$. This has contributions from both the intrinsic molecular T_2 and OD effects. In the absence of OD effects, i.e., when the sample has negligible absorbance or when in the low excitation intensity limit, $T_2^\dagger$ equals T_2 and the photon echo experiment directly measures the intrinsic molecular T_2.

II. THEORY

A. Mathematical formalism

The standard approach to the problem of coherent pulse propagation is a semiclassical density matrix analysis in which the medium is treated quantum mechanically and the field is treated classically.[10] This yields the Maxwell-Optical Bloch equations, a set of four coupled partial differential equations involving the polarization of the medium and the radiation field. Usually the simplification is made that the optical pulse is unchanged by the medium (optically thin sample).[11] This decouples the polarization equations from the field equation and makes their simultaneous solution tractable.

However, some photon echo experiments done to date have been on optically thick samples, and the use of high intensity pulses, short relative to molecular relaxation times, introduces the additional complication of coherent pulse propagation effects, e.g., self-induced transparency and pulse breakup.[12] The fully coupled Maxwell-Optical Bloch (MOB) equations are required to adequately study photon echoes under these conditions.[10,13] Since analytical solutions to the MOB equations are unknown, except under special conditions,[14] we have numerically integrated them and applied them to the photon echo pulse sequence.

The radiation field is assumed linearly polarized along the x direction and propagating along the z axis with frequency ω:

$$\mathbf{E}(z,t) = \mathbf{x}\epsilon(z,t)\cos(\omega t - kz) \ . \tag{1}$$

The two-level medium has energy splitting $\hbar\omega_0$ and its dynamics are described by the Liouville density matrix equation

$$i\hbar(\partial\rho/\partial t) = [\mathcal{H}, \rho] + \text{relaxation terms.} \tag{2}$$

The Hamiltonian is given by $\mathcal{H} = \mathcal{H}_0 + V$, where $\mathcal{H}_0$ is responsible for the $\hbar\omega_0$ splitting and V is the electric dipole interaction

$$V = -\mu E(z,t) \ ,$$

with μ the component of the transition dipole moment operator along the field $\mathbf{E}(z,t)$. The two levels are assumed to be states of definite parity, giving $\mu_{11} = \mu_{22} = 0$. The phases of the states are also chosen such that $\mu_{12} = \mu_{21} = \mu$.

Within this framework, after making the rotating wave approximation and transforming to the rotating frame with the substitution

$$\rho_{21} = \tilde{\rho}_{21}\exp[i(\omega t - kz)] \ , \tag{3}$$

Eq. (2) becomes

$$\frac{\partial\tilde{\rho}_{21}}{\partial t} = \left(i\Delta\omega - \frac{1}{T_2}\right)\tilde{\rho}_{21} - \frac{i\omega_1}{2}(\rho_{22} - \rho_{11}) \ , \tag{4a}$$

$$\frac{\partial\rho_{22}}{\partial t} = \frac{i\omega_1}{2}(\tilde{\rho}_{12} - \tilde{\rho}_{21}) - \frac{(\rho_{22} - \rho_{22}^e)}{T_1} \ , \tag{4b}$$

$$\frac{\partial\rho_{11}}{\partial t} = \frac{i\omega_1}{2}(\tilde{\rho}_{21} - \tilde{\rho}_{12}) - \frac{(\rho_{11} - \rho_{11}^e)}{T_1} \ , \tag{4c}$$

where $\Delta\omega = \omega_0 - \omega$, $\omega_1 = (\mu\epsilon/\hbar)$, and ρ_{ii}^e is the equilibrium value of ρ_{ii}. For our purposes here, relaxation terms are adequately characterized by two phenomenological decay times T_1 and T_2.

Equations (4a)–(4c) can now be cast in the familiar Bloch form[15]:

$$\frac{\partial u}{\partial t} = +\Delta\omega v - \frac{u}{T_2} \ , \tag{5a}$$

$$\frac{\partial v}{\partial t} = -\Delta\omega u + \omega_1 w - \frac{v}{T_2} \ , \tag{5b}$$

$$\frac{\partial w}{\partial t} = -\omega_1 v - \frac{(w - w^e)}{T_1} \ , \tag{5c}$$

where

$$u = 2N\mu\ \mathrm{Re}(\tilde{\rho}_{21}) \ ,$$

$$v = -2iN\mu\ \mathrm{Im}(\rho_{21}) \ ,$$

$$w = N\mu(\rho_{22} - \rho_{11}) \ ,$$

and N is the molecular density.

Equations (5a)–(5c) describe the behavior of the medium in the presence of a radiation field. To complete the analysis, a field equation must be found to account for the effects of the medium back on the field. This is provided by the wave equation derived from Maxwell's equations

$$\frac{\partial^2 E}{\partial z^2} - \frac{n^2}{c^2}\frac{\partial^2 E}{\partial t^2} = \mu_0\frac{\partial^2 P}{\partial t^2} \ , \tag{6}$$

where P is the medium polarization and n is the refractive index of the medium.

So far, the analysis has been general. At this point most analyses assume an optically thin sample. By definition the incident field E_0 that induces the medium polarization P passes through an optically thin sample unchanged. Any field reradiated by the sample as a result of its polarization is negligible compared to E_0, hence cannot modify it. This greatly simplifies the problem. With optically thin samples, P is calculated

using only the incident field. P then serves as a source term in the wave equation to calculate the field reradiated by the medium. This is valid only if the reradiated field is much smaller than the incident field.

To treat short, high intensity pulses in optically thick samples, Eqs. (5) and (6) are made self-consistent by requiring that the E field driven by P in Eq. (6) be the same as that used in Eq. (5) to calculate P.

$P(z,t)$ can be written in the form

$$P(z,t)=\int P(\Delta\omega,z,t)\,g(\Delta\omega)\,d(\Delta\omega)\ , \tag{7}$$

where $g(\Delta\omega)$ is the normalized inhomogeneous line shape function for the transition. Furthermore,

$$P(\Delta\omega,z,t)=N\,\mathrm{Tr}[\rho(\Delta\omega,z,t)\,\mu]=N\mu(\rho_{12}+\rho_{21})\ . \tag{8}$$

Using this result with Eqs. (5) and (7), it follows that

$$P(z,t)=U(z,t)\cos(\omega t-kz)-V(z,t)\sin(\omega t-kx)\ , \tag{9}$$

where

$$U(z,t)=\int u(\Delta\omega,z,t)\,g(\Delta\omega)\,d(\Delta\omega)\ ,$$

and

$$V(z,t)=\int v(\Delta\omega,z,t)\,g(\Delta\omega)\,d(\Delta\omega)\ .$$

Equations (1) and (9) are then substituted into the wave equation (6). Since sine and cosine are linearly independent functions, two equations result. These are simplified by invoking the slowly varying envelope approximation,[18] i.e., $\partial F/\partial t \ll \omega_0 F$, $\partial F/\partial z \ll kF$, $\partial^2 F/\partial t^2 \ll \omega_0(\partial F/\partial z)$, and $\partial^2 F/\partial z^2 \ll k(\partial F/\partial z)$, for $F=\epsilon$, U, and V, successively. The cosine equation is the desired field equation

$$\frac{\partial\epsilon}{\partial z}+\frac{n}{c}\frac{\partial\epsilon}{\partial t}=-\frac{\omega_0 c\mu_0}{2n}V=-\frac{\omega_0 c\mu_0}{2n}\int v(\Delta\omega,z,t)\,g(\Delta\omega)\,d(\Delta\omega)\ . \tag{10}$$

The final step is to perform a change of variables in Eqs. (5) and (6) from (z,t) to (z',t'), where $z'=z$ and $t'=t-(nz/c)$. This gives the basic equations

$$\frac{\partial}{\partial t'}u(\Delta\omega,z',t')=\Delta\omega v-\frac{u}{T_2}\ , \tag{11a}$$

$$\frac{\partial}{\partial t'}v(\Delta\omega,z',t')=-\Delta\omega u+\omega_1 w-\frac{v}{T_2}\ , \tag{11b}$$

$$\frac{\partial}{\partial t'}w(\Delta\omega,z',t')=-\omega_1 v-\frac{(w-w^e)}{T_1}\ , \tag{11c}$$

and

$$\frac{\partial\epsilon}{\partial z'}=-\frac{\omega_0 c\mu_0}{2n}\int v(\Delta\omega,z',t')\,g(\Delta\omega)\,d(\Delta\omega)\ . \tag{12}$$

B. Numerical integration

The set of four coupled partial differential equations (11) and (12) were integrated over a three-dimensional grid having $\Delta\omega$, z', and t' axes. The $\Delta\omega$ axis is only incidental to this discussion, however. The following Adams–Moulton predictor-corrector (PC) pair was used.[17] If $dy/dx=f(x,y)$, then

$$y_n^P=y_{n-1}+(h/2)(3f_{n-1}-f_{n-2})\ ,$$
$$y_n^C=y_{n-1}+(h/2)(f_n+f_{n-1})\ , \tag{13}$$

where h is the step size. This PC pair requires function values at two previous grid points. This presents no problems for the polarization functions [Eq. (11)] which are propagated through time and are known at any $t'\le 0$. However, $\epsilon(z',t')$ is known only at the $z'=0$ plane for $t'>0$, i.e., $\epsilon(0,t')$ represents the incoming pulse shape. Since $\epsilon(z',t')$ is propagated through space by Eq. (12), the field must be determined along the grid points adjacent to the $z'=0$ plane (i.e., points in the $z'=1$ plane) before Eq. (13) can be applied. This was done by using the following PC pair:

$$y_n^P=y_{n-1}+hf_{n-1}\ ,$$
$$y_n^C=y_{n-1}+(h/2)(f_n+f_{n-1})\ . \tag{14}$$

The entire grid can be covered in a number of ways. We chose to cover it by taking a step along t', traversing z' (starting at $z'=0$) for this t' value, taking another step along t', traversing z', and so forth. In traversing z', since $\epsilon(0,t')$ is known, the polarization at $(0,t')$ was calculated using Eq. (13). Then ϵ and the polarization were simultaneously calculated at $(1,t')$ using Eqs. (14) and (13), respectively. For $z'>1$, Eq. (13) was used for both the field and the polarization.

C. Program and calculated results

A computer program was developed to perform the photon echo calculation described above. The program calculates the effects of optically dense samples on echo decays. Qualitatively, the calculation works in the following manner: a hypothetical crystal of fixed concentration and thickness is divided into many thin slices (z' axis). The Gaussian inhomogeneous line of the molecules in each slice is divided into many separate isochromats ($\Delta\omega$ axis). Each Gaussian excitation pulse is assumed cut into many thin rectangular slices with an overall Gaussian envelope (t' axis). The first excitation pulse coherently pumps the sample using the complete treatment of Eqs. (11) to (14). After the first excitation pulse, i.e., during the first period τ, the complete treatment is still applied for the time development of the sample polarization until the polarization has effectively decayed to zero, i.e., throughout the free induction decay. At this time, the usual uncoupled density matrix transformation of each individual isochromat suffices to continue the time development for the rest of the period τ. The full MOB treatment is again applied during the second excitation pulse. During the inhomogeneous rephasing and echo formation, the uncoupled density matrix transformation is again employed unless the sample polarization becomes large enough to warrant the use of the complete formalism. For small echo E fields, reabsorption of the echo (at frequency ω_0) is calculated as it passes through each crystal slice and the absorption coefficient is proportional to the w component of the $\omega=\omega_0$ isochromat for different crystal slices. The time-integrated echo intensity at the far side of the sample is then calculated. This sequence is repeated for different excitation pulse separations giving an echo decay. Care is taken during

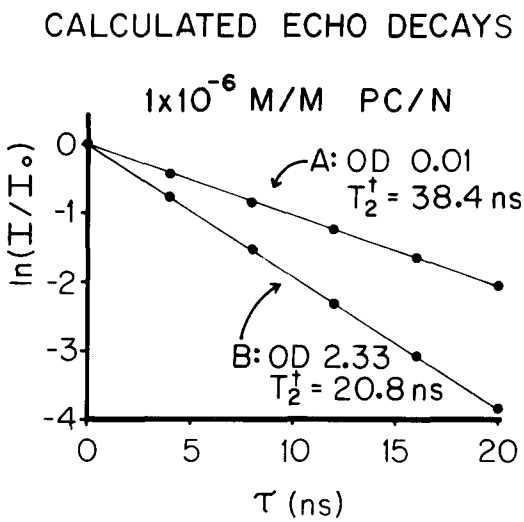

FIG. 1. Calculated photon echo decays for two hypothetical 1×10^{-6} M/M pentacene in naphthalene crystals (dots are calculated points). Sample A is 1.3 μm thick with peak OD 0.01. Sample B is 300 μm thick with peak OD 2.33. Both samples are identical ($T_1 = 19.2$ ns, $T_2 = 2T_1$, $\mu = 0.7$ D, inhomogeneous linewidth = 40 GHz except for thickness. Due to optical density effects, the thicker sample B yields an echo decay, $T_2^\dagger$, which is much faster than the intrinsic molecular T_2. Sample A, with low OD, yields $T_2^\dagger = T_2$.

each step to ensure self-consistency of the iterated E field and sample polarization and that sample slices, inhomogeneous line slices and temporal envelope slices of the excitation pulses and echo pulse are fine enough to assure accurate results.

An example of calculated photon echo decays is presented in Fig. 1 for two hypothetical samples of pentacene in naphthalene ($\mu \approx 0.7$ D for $S_0 \rightarrow S_1$, $T_1 = 19.2$ ns and assuming $T_2 = 2T_1$) of concentration 10^{-6} M/M and inhomogeneous linewidth of 40 GHz. Excitation pulses of length 30 ps and areas $\pi/2$ and π were used to match photon echo experiments. The first crystal was 1.3 μm thick with a peak OD of 0.01. This crystal gave an echo decay (labeled A in Fig. 1) of 38.4 ns which is exactly $2T_1$. This sample is in the low OD limit. The second crystal was 300 μm thick, hence had a peak OD of 2.33. The echo decay time of this sample is 20.8 ns, which is considerably faster than $2T_1$, yet the only difference in the two calculations is the thickness, hence the optical density, of the samples. For the first sample, neither pulse was affected enough to noticeably change its area on passing through the sample. In the second sample, however, the first excitation pulse had decayed in area from $\pi/2$ to 0.36π. The area of the second excitation pulse changed from π to 0.99π and 0.95π for interpulse separations τ of 2 and 20 ns, respectively. This illustrates the time dependence of the evolution of the second excitation pulse. Figure 2 illustrates the calculated OD dependence of $T_2^\dagger$ for various ODs. The results are identical regardless of whether the thickness or concentration of the sample is varied.

Results of a calculation of the dependence of the photon echo decay rate upon the intensity of the excitation pulses is shown in Fig. 3. The ratio of excitation pulse areas was kept constant at 1 : 2. The low OD crystal, independent of excitation intensities, yields $T_2^\dagger = 2T_1 = 38.4$ ns. However, for a $\pi/2 - \pi$ pulse sequence, the high OD crystal gave a much faster $T_2^\dagger$. As the excitation pulse intensities decrease, the $1/T_2^\dagger$ values initially increase, then decrease and eventually level off to $T_2 = 2T_1$ at very low intensity. The maximum calculated value for $1/T_2^\dagger$ occurs for excitation pulses with areas of about $\pi/3$ and $2\pi/3$. If the average degree of excitation in the sample is greater than 50%, the echo pulse will experience a net gain. For $\tau \ll T_1$, this will generally be the case if $\cos(\theta_1 + \theta_2) < 0$. For long τ values, the sample will become absorbing again due to T_1 processes. The decays in these cases tended to be nonexponential at first, becoming exponential at long τ values.

These calculations indicate that one should expect to observe a dependence of echo decay rate upon the OD of the sample. Additionally, a decrease in the echo decay rate with decrease in excitation pulse intensity is expected and, in the low power limit, the decay due to intrinsic molecular dephasing processes is obtained.

III. EXPERIMENTAL SECTION

The picosecond photon echo system used in these experiments has been described in detail previously.[7,18]

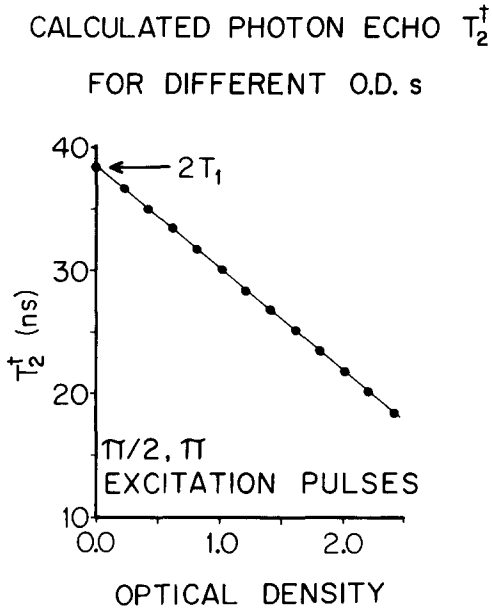

FIG. 2. Calculated dependence of the echo decay $T_2^\dagger$ on the sample OD (dots are calculated points). Echo decays were calculated for hypothetical 1.0×10^{-6} M/M PC/N crystals with different thicknesses (hence different OD's). Parameters are those given in the caption of Fig. 1. This figure shows the strong effect sample OD can have on the echo decay time. It can be seen that under high power excitation conditions ($\pi/2$, π), the intrinsic molecular T_2 is obtained only in the zero OD limit. When crystal thickness was held constant and the concentration varied to generate the same set of ODs, identical results were obtained.

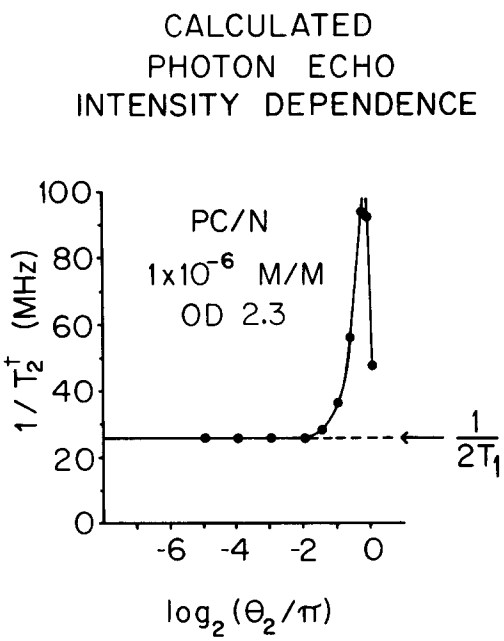

FIG. 3. Calculated dependence of photon echo decay rate $T_2^\dagger$ upon intensity of excitation pulses. Ratio of areas of excitation pulses was 1 : 2 (intensity ratio 1 : 4) in all calculations. A low OD sample yields the intrinsic molecular T_2 ($T_2 = 2T_1$) for all excitation intensities. A high OD sample yields the curve shown. The peak in the curve is discussed in the text. At low excitation intensities, the calculations predict that OD effects are eliminated and the intrinsic molecular T_2 can be obtained from the echo decay measurement.

Excitation pulses are generated by a mode-locked, cavity-dumped dye laser synchronously pumped by the frequency-doubled output of a cw-pumped, acousto-optically mode-locked and Q-switched Nd:YAG laser. This dye laser system provides a very stable source of 30 ps, 20 μJ pulses at a 400 Hz repetition rate.

A dye laser single pulse is split into two and appropriate temporal delays are introduced with a motorized optical delay line. The two excitation pulses are directed to the sample located in a liquid He Dewar. The generated echo signal leaves the sample and is temporally, spatially and frequency separated from the excitation pulses by summing with a single, 80 ps IR pulse. The up-converted echo signal is then lock-in detected. Most of the echo decays were recorded using collinear excitation pulses. Some decays were obtained using crossed excitation pulses and echo pulses were still detected by frequency summation.

The ratio of the excitation pulse intensities was set to 1 : 4 (1 : 2 pulse area ratio) with a variable filter in one beam. For studies of the dependence of echo decay rate upon excitation intensity, the excitation pulse energies were measured before and after each set of decays with a photodiode and calibrated filters. This ensured that no changes in laser intensity occurred on a short term basis and that slight day-to-day fluctuations in intensity could be accounted for.

The pentacene in naphthalene crystals used were grown from the melt by the Bridgman technique using only thoroughly zone-refined naphthalene. The pentacene, obtained from Aldrich, was used without further purification. Cut samples of the best optical quality were used. The $S_0 \rightarrow S_1$ pentacene transition in naphthalene is strongly b-axis polarized.[19] In mounting samples on 600 μm pinholes for an experiment, a conoscopic microscope with crossed polarizers was used to locate the optic axes to ensure that the crystal b axis was parallel to the laser polarization. Crystal concentrations were accurately measured from b axis polarized absorption spectra.

A calibrated Datametrics Barocel manometer was used in the measurements of the temperature dependence of echo decays. With it, liquid He temperatures were measured to within ± 0.02 K.

IV. RESULTS AND DISCUSSION

A. OD dependence of eacho decays

Figure 4(a) shows photon echo decays of two crystals of pentacene in naphthalene, each with thickness ~ 400

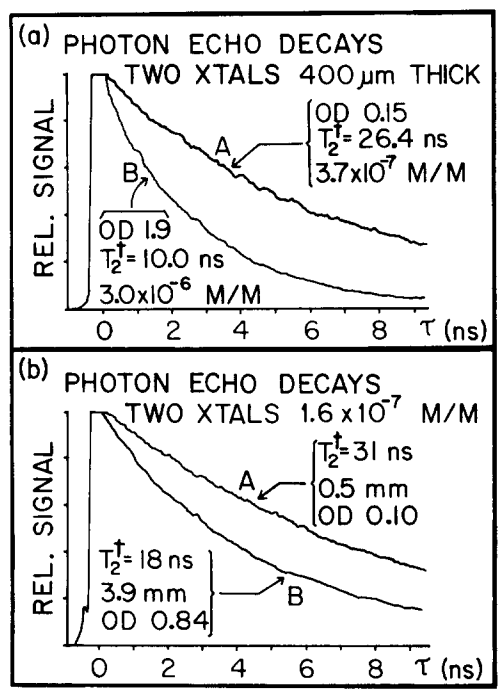

FIG. 4. Experimental photon echo decay data taken with ~ $\pi/2$, π excitation pulses on pentacene in naphthalene crystals. (a) Slow echo decay of low concentration crystal (A) and faster echo decay of more concentrated crystal (B). Evidence such as this was previously interpreted as a concentration dependence. (b) Both decays are for crystals having identical concentration $C = 1.6 \times 10^{-7}$ M/M, but crystal B has approximately eight times the OD. The high OD crystal gives a faster echo decay under high power excitation conditions although the concentrations are identical. This demonstrates that differences in echo decays are due to optical density effects *not* concentration effects.

μm. The curve labeled A is of a crystal with concentration 4×10^{-7} M/M and maximum OD 0.15. That labeled B is of a crystal with concentration 3×10^{-6} M/M and maximum OD 1.9. Both decays were taken with the same excitation intensity (pulse areas $\sim\pi/2$, π), yet the higher OD crystal yielded a much faster decay. Evidence such as this was previously interpreted as a concentration dependence of the echo decay rate.[7] That this is not the case is illustrated in Fig. 4(b) in which photon echo decay data (same excitation intensity) are displayed for two crystals, both of 1.6×10^{-7} M/M concentration but of different thickness. The thin crystal (labeled A) was 500 μm thick (max OD = 0.096) and produced an echo decay with $T_2^{\dagger}=31.2$ ns. The thick crystal (labeled B) was 3900 μm thick (max OD = 0.84) and $T_2^{\dagger}=18.0$ ns. The fact that crystals with identical concentrations but different ODs give different decay rates conclusively demonstrates that decay rate differences do not arise from concentration effects, but rather from OD effects. The high OD sample acts strongly on the sample in a manner which depends upon τ, the time between the pulses. This results in faster decays in high OD samples. These fast decays do not arise from intrinsic molecular properties, but from the effect that strong coupling between the field and the sample has on the photon echo observable.

It had been proposed previously[7,8] that the fast decays were due to long range dipole–dipole interactions between impurity molecules. In a recent, theoretical study,[20] Skinner *et al.* have shown that the various dipole–dipole mechanisms[7,8] should not be significant in these experiments.

Samples with high ODs were observed to exhibit highly intensity-dependent echo decay rates. This is illustrated in Fig. 5(a). Two successive echo decays performed on the same sample are presented. The faster decay was obtained at high excitation intensity, corresponding to $\pi/2$ and π pulses. The slower decay was obtained with the excitation intensity reduced to pulse areas of $\pi/32$ and $\pi/16$. Results of a study of the intensity dependence of echo decay rate are presented in Fig. 5(b) for several of the crystals studied. For high OD samples, the decay rate becomes slower as the excitation pulse intensities are decreased. Low OD samples give intensity independent decays, as predicted by theory. The most important feature is the fact that *the decay rates for all crystals, regardless of OD or concentration, become equal at very low excitation intensities*. For the pentacene in naphthalene crystals studied here, the low-intensity limiting T_2 for high OD, high concentration samples appears to be the same as that obtained for low OD, low concentration samples: T_2 = 32 ns and $T_2\neq 2T_1$. This is discussed in detail below.

The experimental intensity dependence shown in Fig. 5, although qualitatively in agreement with theory is quantitatively different from that calculated in Fig. 3. This might be explained by the fact that the actual excitation pulses are not completely transform limited. The excitation pulses are not Gaussian in temporal profile and are not constant amplitude plane waves as they advance through the sample. The sample pinholes reduce but do not completely eliminate the Gaussian transverse beam profile and crystal imperfections cause additional distortions of the intensity profile. The nonideal excitation pulses will not uniformly excite the sample, the net result of which may be to smooth out the peak in the calculated intensity dependence of Fig. 3.

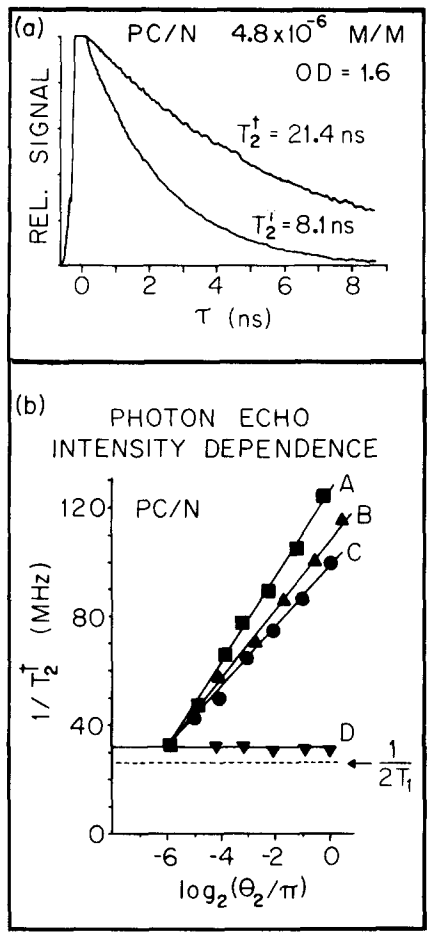

FIG. 5. (a) Two experimental echo decays taken on the same crystal of pentacene in naphthalene at different excitation intensities. The fast decay (8.1 ns) is observed for $\sim\pi/2$, π excitation pulses and the slower decay (21.4 ns) is observed at lower excitation energy ($\sim\pi/32$, $\pi/16$). This is consistent with theoretical predictions. (b) Dependence of experimental echo decay rate upon excitation intensity. Curve D(OD = 0.1) is intensity independent as predicted by theory for a low OD crystal and therefore the echo decay gives the intrinsic molecular T_2. Note that $T_2\neq 2T_1$ even under low OD and low power conditions. Curves A, B, and C show a strong dependence of the echo decay rate on intensity as predicted by theory for high OD crystals. (A: OD = 1.6; B and C: OD = 1.1.) The data appears to be consistent with the theoretical prediction that in the limit of low power excitation, the intrinsic molecular T_2 is obtained from high OD crystals.

In the introduction, it was noted that the second excitation pulse and echo pulse experience inherently different sample excitation environments at different values of τ in an optically thick sample. At high excitation intensities, a sizable w component is created in the sam-

ple. This w component decays with time resulting in a large change in w over the time period τ. For an optically dense sample, the pulses evolve a great deal in area, shape and energy, as they propagate through the sample. The large change in w with τ causes a large change in the absorbance of the sample with τ. This causes significant differences in the evolution of the second excitation pulse and echo pulse for different times τ. In the low excitation limit, the sample molecules are essentially in the ground state at all times. Hence, the second excitation pulse and echo pulse encounter an effectively identical sample regardless of τ. Thus, the effect of differing absorbances for different τ values disappears and the intrinsic molecular T_2 is measured.

In some samples with identical high ODs, and different concentrations (different thicknesses) under high power excitation, different decay times were observed. This can be qualitatively explained as follows: the portion of each sample excited is a cylinder with diameter equal to that of the sample pinhole and length equal to the crystal thickness. During the photon echo pulse sequence, some spontaneous emission of photons occurs. These photons have some probability of stimulating the emission of other photons. Both types of emission prevent molecules from contributing to the signal and will increase the echo decay rate. Stimulated emission will be greater for the higher concentration sample since spontaneously emitted photons moving obliquely to the excited cylinder axis experience a higher absorbance. The increased stimulated emission in the higher concentration sample will cause a faster echo decay. Here too, as above, the enhanced decay vanishes at sufficiently low excitation intensities since all molecules are essentially in the ground state.

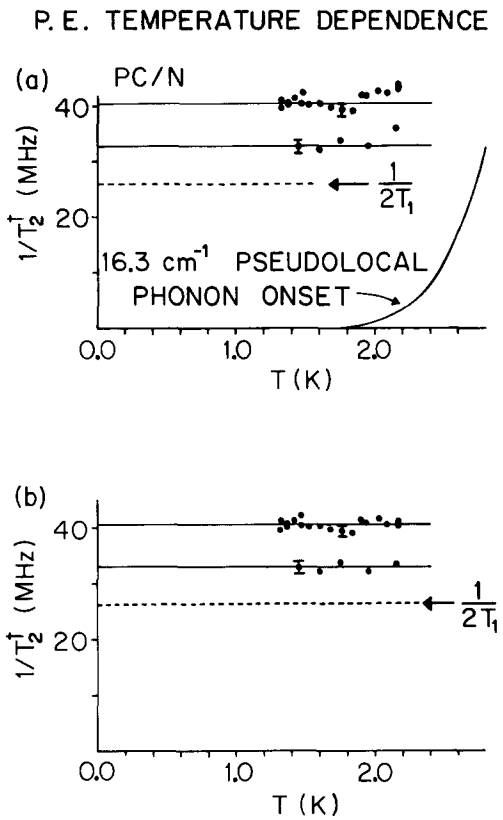

FIG. 6. Temperature dependence of the echo decay rate for two crystals. Part (a) shows the raw data. The upper data set is for a crystal near the low OD limit, while the lower data set is for a crystal in the low OD limit. The contribution to $1/T_2^\dagger$ due to the well characterized 16.3 cm^{-1} pseudolocal phonon[19] is subtracted to give the data in part (b) of the figure. Part (b) demonstrates that $T_2^\dagger$ is temperature independent at very low temperature and differs from $2T_1$ even at 0 K.

B. The low temperature T_2

In the pentacene in naphthalene experiments, both high and low concentration samples having either high or low OD exhibit a low power limiting echo decay time of $T_2 = 32$ ns which differs significantly from $2T_1 = 38.4$ ns.[7] A temperature dependence study of the low OD limit T_2 was performed over the temperature range 1.32 to 2.17 K (see Fig. 6). A slight rise at the high end of the temperature range studied is attributable to the thermal onset of a 16.3 cm^{-1} pseudolocal phonon mode which has been well characterized at higher temperatures.[19] The contribution of the pseudolocal phonon to the echo decay rate becomes vanishingly small below 2 K and cannot account for the temperature independent decay with $T_2 \neq 2T_1$ observed between 1.3 and 2 K.

Theoretical models of phonon induced homogeneous line broadening predict only lifetime broadening at 0 K (i.e., $T_2 = 2T_1$) and a strong temperature dependence to any phonon induced broadening above 0 K. For example, quadratic coupling of the transition to acoustic phonons should give a T^7 temperature dependence.[21] Even over the limited temperature range studied, a T^7 temperature dependence would result in a more than 30-fold change in the nonlifetime broadening. Because there is some scatter in the measurements made at various temperatures, we cannot completely rule out a very mild (perhaps linear or less) temperature dependence. Theoretical models of phonon-induced line broadening all predict a much stronger temperature dependence than could possibly be consistent with the data.

The homogeneous line shape is the Fourier transform of the equilibrium dipole moment correlation function

$$I(\omega) \propto \int_{-\infty}^{\infty} dt\, e^{i\omega t} \langle \hat{\mu}(t)\, \hat{\mu}(0) \rangle_0 \ . \tag{15}$$

The usual assumption, arising out of the phenomenological Bloch equations, is that the photon echo decay is the Fourier transform of the line shape, i.e., it is determined by the correlation function $\langle \hat{\mu}(t)\, \hat{\mu}(0) \rangle_0$, a two operator, two time equilibrium correlation function. For some systems, this is indeed the case. However, in a recent paper,[9] Skinner *et al.* presented a correlation function analysis of the photon echo and other coherent optical transients for a quasi-two-level system. A quasi-two-level system is one in which, in general, a ground state manifold of levels is coupled by transition moments to an excited state manifold. The manifold must have a finite width but can be discrete or continuous. The model assumes short excitation pulses and

an initially Boltzmann distribution of population in the ground state manifold. With these conditions the photon echo amplitude was shown to be

$$\tilde{P}(2\tau) = -i\langle \sin[B_1\hat{\mu}(-\tau)]\sin[B_2\hat{\mu}(0)] \times \hat{\mu}(\tau)\sin[B_2\hat{\mu}(0)]\cos[B_1\hat{\mu}(-\tau)]\rangle_0 \ , \quad (16)$$

where

$$B_i = E_i t_i/2\hbar$$

and E_i and t_i are the electric field and the duration of the ith pulse, respectively. This is a five operator three time equilibrium correlation function, in contrast to the line shape correlation function. In some situations, the photon echo correlation function gives the same results as traditional line shape theory. However, in general the echo correlation function is different from that arising out of line shape theory and will not decay in the same manner.

The quasi-two-level system studied theoretically is, in many respects, closely analogous to the pentacene in naphthalene system. The ground state S_0 and the excited state S_1 of an isolated pentacene molecule form a two-level system (the bare excitation) coupled by a transition moment. When placed in the naphthalene host, the S_0 and S_1 states each couple to the naphthalene lattice phonons. Some of the transition moment is carried into the mixed pentacene phonon states. Thus, the ground and excited states are really manifolds of states. Experimentally this is manifested in the existence of the phonon sideband observed in this system.

The pentacene in naphthalene experiments do not meet the conditions of the theory of Skinner *et al.* The width of the phonon manifold is infinite since multiple excitation of phonons allows any amount of lattice energy to be present, while the theory requires a finite width manifold. Additionally, the theory as developed requires that excitation pulses be short relative to the inverse of the width of the phonon manifold. The excitation pulses used in the experiments were 30 ps in length. This is far longer than the inverse of the Debye frequency (~ 66 cm^{-1}), which is the minimum conceivable manifold width. Nonetheless, the results of Skinner *et al.* demonstrate that there is no *a priori* reason to believe that the photon echo decay is directly related to the homogeneous line shape in a complex system, e.g., any quasi-two-level system. Consequently, the traditional result of line shape theory, that T_2 need equal $2T_1$ at 0 K, is not necessarily a foregone conclusion for quasi-two-level systems, since the correlation function describing the photon echo in general is different from the line shape correlation function.

If the above considerations are important for the pentacene in naphthalene system, then the net result is that $T_2 \neq 2T_1$ because of the inherent temperature independent multilevel structure of the system. Skinner *et al.*[9] have shown that it is not safe to assume that a photon echo decay is governed by the same correlation function that determines the optical homogeneous linewidth. However, the correlation function treatment of the echo is currently only applicable to a limited set of situations. A full understanding of this experimental system may require the extension of the theoretical treatment to a broader class of experimentally realizable conditions.

V. CONCLUDING REMARKS

In this paper, we have examined experimentally and theoretically the effects of optical density on the decay of photon echoes. For optically thick samples, it is found necessary to use coupled Maxwell-Optical Bloch equations to adequately understand the time dependence of photon echo decays. For high intensity excitation pulses, the echo decays are not determined strictly by molecular dynamics but also depend upon the sample's effect on the radiation field. It is pointed out that previously reported concentration dependent echo decays which had been ascribed to intermolecular interactions, are actually optical density effects.

A significant result, found both experimentally and theoretically, is that in the limit of low excitation intensities, the optical density effects are eliminated from the echo decays and intrinsic molecular properties can be examined. Echo decay data for pentacene in naphthalene is found to be temperature independent, but with $T_2 \neq 2T_1$. It was suggested that recent theoretical work describing the photon echo in terms of equilibrium correlation functions which differ from the usual correlation function which describes the homogeneous linewidth may contain the seed of an explanation for the temperature independent difference between T_2 and $2T_1$.

ACKNOWLEDGMENTS

We would like to thank Professor James L. Skinner, Chemistry Department, Columbia University and Professor Hans C. Andersen, Chemistry Department, Stanford University for many helpful discussions and critical comments relating to this work. We would also like to thank the National Science Foundation (DMR-79-20380) for support of this research.

[1] I. D. Abella, N. A. Kurnit, and S. R. Hartmann, Phys. Rev. **141**, 391 (1966); W. H. Hesselink and D. A. Wiersma, Chem. Phys. Lett. **56**, 227 (1978); R. W. Olson, F. G. Patterson, H. W. H. Lee, and M. D. Fayer, *ibid.* **77**, 403 (1981).

[2] W. B. Mims, in *Electron Paramagnetic Resonance*, edited by S. Geschwind (Plenum, New York, 1972); E. L. Hahn, Phys. Rev. **77**, 297 (1950); N. A. Kurnit and S. R. Hartmann, in *Interaction of Radiation With Solids*, edited by A. Bishay (Plenum, New York, 1967); W. H. Hesselink and D. A. Wiersma, Chem. Phys. Lett. **50**, 51 (1978).

[3] T. C. Farrar and E. D. Becker, *Pulse and Fourier Transform NMR* (Academic, New York, 1971).

[4] R. P. Feynman, F. L. Vernon, Jr., and R. W. Hellwarth, J. Appl. Phys. **28**, 49 (1957).

[5] S. L. McCall and E. L. Hahn, Phys. Rev. **183**, 457 (1969); D. J. Kaup, Phys. Rev. A **16**, 704 (1977) and references therein; F. A. Hopf, G. L. Lamb, Jr., C. K. Rhodes, and M. O. Scully, *ibid.* **3**, 758 (1971), and references therein.

[6] P. W. Anderson, Phys. Rev. **109**, 1492 (1958); P. W. Anderson, Comments Solid State Phys. **2**, 193 (1970); J. Koo, L. R. Walker, and S. Geschwind, Phys. Rev. Lett. **35**, 1669 (1975).

[7] D. E. Cooper, R. W. Olson, and M. D. Fayer, J. Chem. Phys. **72**, 2332 (1980).

[8] J. B. W. Morsink, B. Kruizinga, and D. A. Wiersma, Chem.

Phys. Lett. **76**, 218 (1980).
[9]J. L. Skinner, H. C. Andersen, and M. D. Fayer, Phys. Rev. A (to be published).
[10]M. Sargent III, M. O. Scully, and W. E. Lamb, Jr., *Laser Physics* (Addison-Wesley, Reading, Mass., 1974); L. Allen and J. H. Eberly, *Optical Resonance and Two-Level Atoms* (Wiley, New York, 1975); R. G. Brewer, in *Frontiers in Laser Spectroscopy*, edited by R. Balian, S. Haroche, and S. Liberman (North-Holland, Amsterdam, 1977), p. 341.
[11]R. L. Shoemaker, in *Laser and Coherence Spectroscopy*, edited by J. I. Steinfeld (Plenum, New York, 1978), p. 197; R. G. Brewer and R. L. Shoemaker, Phys. Rev. Lett. **27**, 631 (1971).
[12]S. L. McCall and E. L. Hahn, Phys. Rev. Lett. **18**, 908 (1967); Phys. Rev. **183**, 457 (1969); A **2**, 861 (1970).
[13]A. Yariv, *Quantum Electronics*, 2nd ed. (Wiley, New York, 1975), p. 388.
[14]A. Icsevgi and W. E. Lamb, Jr., Phys. Rev. **185**, 517 (1969).
[15]F. Bloch, Phys. Rev. **70**, 460 (1946).
[16]J. A. Armstrong and E. Courtens, IEEE J. Quantum Electron. **QE4**, 411 (1968); **QE5**, 249 (1969).
[17]G. Dahlquist and Å. Björk, *Numerical Methods*, translated by N. Anderson (Prentice-Hall, Englewood Cliffs, 1974).
[18]D. E. Cooper, R. W. Olson, R. D. Wieting, and M. D. Fayer, Chem. Phys. Lett. **67**, 41 (1979).
[19]W. H. Hesselink and D. A. Wiersma, J. Chem. Phys. **73**, 648 (1980).
[20]J. L. Skinner, H. C. Andersen, and M. D. Fayer, J. Chem. Phys. **75**, 3195 (1981).
[21]B. DiBartolo, *Optical Interactions in Solids* (Wiley, New York, 1968); K. E. Jones and A. H. Zewail, in *Advances in Laser Chemistry*, edited by A. H. Zewail (Springer, New York, 1978).